THE JOURNAL OF PHYSICAL CHEMISTRY B
A JOURNAL OF THE AMERICAN CHEMICAL SOCIETY

pubs.acs.org/JPCB

Article

Hydronium Ions Are Less Excluded from Hydrophobic Polymer–Water Interfaces than Hydroxide Ions

Ryan L. Myers,[#] Aoi Taira,[#] Chuanyu Yan, Seung-Yi Lee, Lauren K. Welsh, Patrick R. Ianiro, Tinglu Yang, Kenichiro Koga,* and Paul S. Cremer*

Cite This: *J. Phys. Chem. B* 2025, 129, 726–735

Read Online

ACCESS | Metrics & More | Article Recommendations | Supporting Information

ABSTRACT: The cloud point temperatures of aqueous poly(*N*-isopropylacrylamide) (PNIPAM) and poly(ethylene) oxide (PEO) solutions were measured from pH 1.0 to pH 13.0 at a constant ionic strength of 100 mM. This ionic strength was reached by mixing the appropriate concentration of NaCl with either HCl or NaOH. The phase transition temperature of both polymers was nearly constant between pH 2.0 and 12.0. However, the introduction of 100 mM HCl (pH 1.0) led to an increase in the cloud point temperature, although this value was still lower than the cloud point temperature in the absence of salt. By contrast, the introduction of 100 mM NaOH (pH 13.0) caused a decrease in the cloud point temperature, both relative to adding 100 mM NaCl and adding no salt. Nuclear magnetic resonance (NMR) studies of these systems were performed below the cloud point temperature, and the chemical shifts closely tracked the corresponding changes in the phase transition temperature. Specifically, the introduction of 100 mM HCl caused the ^{1}H chemical shift to move downfield for the CH resonances from both PNIPAM and PEO, while 100 mM NaOH caused the same resonances to move upfield. Virtually no change in the chemical shift was seen between pH 2.0 and 12.0. These results are consistent with the idea that a sufficient concentration of H_3O^+ led to polymer swelling compared to Na^+, while substituting Cl^- with OH^- reduced swelling. Finally, classical all-atom molecular dynamics (MD) simulations were performed with a monomer and 5-mer corresponding to PNIPAM. The results correlated closely with the thermodynamic and spectroscopic data. The simulation showed that H_3O^+ ions more readily accumulated around the amide oxygen moiety on PNIPAM compared with Na^+. On the other hand, OH^- was more excluded from the polymer surface than Cl^-. Taken together, the thermodynamic, spectroscopic, and MD simulation data revealed that H_3O^+ was less depleted from hydrophobic polymer/water interfaces than any of the monovalent Hofmeister metal cations or even Ca^{2+} and Mg^{2+}. As such, it should be placed on the far-right side of the cationic Hofmeister series. On the other hand, OH^- was excluded from the interface and could be positioned in the anionic Hofmeister series between $H_2PO_4^-$ and SO_4^{2-}.

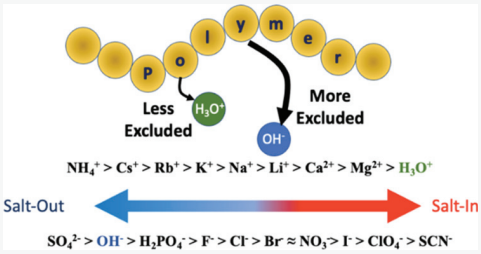

INTRODUCTION

In 1888, Franz Hofmeister ranked common salt ions according to their ability to salt egg white proteins out of solution.[1] Since then, cations and anions have been found to follow a recurring series for a wide range of physical and chemical phenomena. This includes everything from polymer solubility and protein denaturation to micelle formation and catalytic turnover.[2−7] Ions on the left side of the Hofmeister series have typically been found to precipitate polymers, proteins, and supramolecular structures out of solution via an excluded volume mechanism, whereas ions on the right side, salt these same organic species into solution through ion-macromolecule interactions.[8] In the latter case, weakly hydrated anions bind to hydrophobic regions of uncharged organic molecules because the displacement of the hydration shells is thermodynamically favorable. Metal cations typically do not show this type of behavior and instead interact with negatively or partially negatively charged regions on organic functional groups.[9] Figure 1a shows the consensus Hofmeister series for thermal responsive polymers that display a lower critical solution temperature (LCST) and have only a modest number of polar or charged groups.

Until now, neither OH^- nor H_3O^+ have been ranked in the anionic or cationic Hofmeister series, respectively, for uncharged polymers displaying an LCST in water. There have, however, been attempts to place these ions into the series by following the behavior of soluble proteins and related aqueous systems.[4,10] This is quite challenging, especially for molecules that present charged functional groups. In fact, charged groups like carboxylic acids, phosphates, phosphonates, sulfates, sulfonates, amines, guanidine, and histidine are protonated at sufficiently low pH, but become deprotonated at higher pH values. The precise apparent pK_A values vary with

Received: August 26, 2024
Revised: December 15, 2024
Accepted: December 20, 2024
Published: December 31, 2024

https://doi.org/10.1021/acs.jpcb.4c05748
J. Phys. Chem. B 2025, 129, 726–735

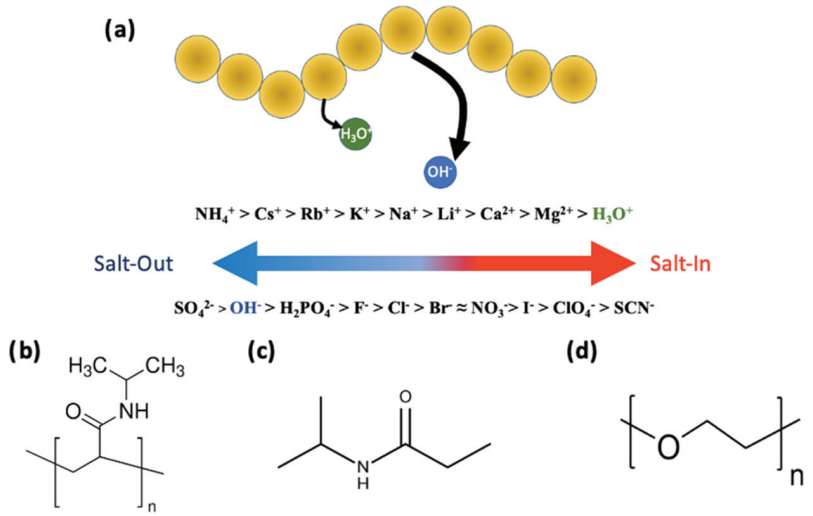

Figure 1. (a) Slight exclusion of H_3O^+, and the greater exclusion of OH^- from the polymer/water interface (yellow spheres represent a polymer molecule). (b) The molecular structures of poly(*N*-isopropylacrylamide) (PNIPAM) (c) the PNIPAM-like monomer (NIPPA) without the double bond and (d) poly(ethylene oxide) (PEO). It should be noted that all the polymers studied herein display an LCST. They are hydrophobically hydrated and collapse on entropic grounds. As such, although they are amphiphilic macromolecules, they are referred to as hydrophobic polymers herein.

the concentration of other salts in solution in an ion specific fashion.[11−13] Therefore, it is usually challenging to dissever Hofmeister series effects for H_3O^+ and OH^- from those involving the charged state of the macromolecule. Another concern with modulating the pH is the hydrolysis of key functional groups. For example, peptide bonds are hydrolyzed at both basic and acidic extremes, and this problem constrains the pH range that can be explored.

By contrast with protein and polymer solubility, H_3O^+ and OH^- ions have been more intensively studied in electrolyte solutions[14,15] or at hydrophobic interfaces such as the air/water and oil/water interfaces.[16−26] It has been shown that the surface tension of the air/water interface decreases when HCl is introduced into solution. Given the fact that Cl^- is neither strongly partitioned toward or away from the air/water interface, this suggests that H_3O^+ should be enriched there.[27−29] On the other hand, NaOH increases the surface tension which has been taken to imply that both Na^+ and OH^- are excluded from the air/water interface.[18,30] Moreover, most studies find that changing the identity of the metal cation has little influence on surface tension.[10,31] This fact would also suggest that OH^- should be excluded from the air/water interface. These interpretations of the surface tension trends for H_3O^+ and OH^- have been supported by ζ-potential measurements as well as spectroscopic data from sum frequency generation (SFG), second harmonic generation (SHG), infrared (IR), Raman, and photoelectron spectroscopy experiments.[16−25,32−40] MD simulations and density functional theory (DFT) calculations also support these ideas.[18,37,41,42] Moreover, Voth and co-workers suggested that the lone pair on H_3O^+ is a poor hydrogen bond acceptor, whereas the three hydrogens are good hydrogen bond donors.[43] As such, H_3O^+, to the extent that it exists, should orient at the air/water interface so that its lone pair faces the air, while the hydrogens point downward into the solution. Very recent SFG measurements indicate that H_3O^+ displaces water molecules with a dangling OH at the interface.[28]

Not all of the available evidence necessarily favors the idea that H_3O^+ accumulates at the air/water interface, while OH^- is strictly excluded. DFT calculations from Mundy and co-workers found that isolated OH^- and H_3O^+ ions have little preference for partitioning toward or away from the air/water interface.[44] Moreover, Mondal and Shen concluded that OH^- was enriched at the air/water interface in the presence of longer chain fatty alcohol monolayers.[45,46] Other methods, including high pH ζ-potential measurements, thin aqueous film stability measurements, electrophoretic measurements, as well as MD simulations at rigid walls suggest that neither OH^- nor H_3O^+ accumulates at hydrophobic surfaces.[16,26,37−39,47]

In this study, we have explored the enrichment/depletion of H_3O^+ and OH^- at the polymer/water interface using Cl^- and Na^+ as the respective counterions. These investigations were performed with poly(*N*-isopropylacrylamide) (PNIPAM) at a molecular weight of 186,000 Da and with poly(ethylene oxide) (PEO) at a molecular weight of 900,000 Da (Figure 1b,d). Both polymers are thermoresponsive and precipitate out of water above their respective cloud point temperatures. Employing PNIPAM at a concentration of 10 mg/mL (approximately 80 mM in monomer units) in neat water leads to precipitation as a solid just above 31 °C. Like other acrylamides, PNIPAM consists of a hydrocarbon backbone and has an amide moiety on its side chain. The NH groups on small molecule amides do not deprotonate until well above pH 15 and the carbonyl oxygen has a pK_A of approximately −0.5.[48] By comparison, 10 mg/mL PEO (approximately 230 mM in monomer units), which has a cloud point temperature near 95 °C, should be even more stable in acidic solutions. Indeed, dimethyl and diethyl ether cannot be protonated until approximately a of pH −2.5.[49,50] Moreover, ethers have no functional groups to deprotonate under basic conditions. As such, both PNIPAM and PEO remain nearly uncharged and stable between pH 1.0 and 13.0.

Herein, a combination of cloud point measurements, NMR spectroscopy, and all-atom MD simulations with classical force fields was performed. The results indicated that both H_3O^+ and OH^- were excluded from the PNIPAM/water and PEO/water interfaces, at least up to a concentration of 100 mM. Nevertheless, the data were consistent with the notion that

https://doi.org/10.1021/acs.jpcb.4c05748
J. Phys. Chem. B 2025, 129, 726−735

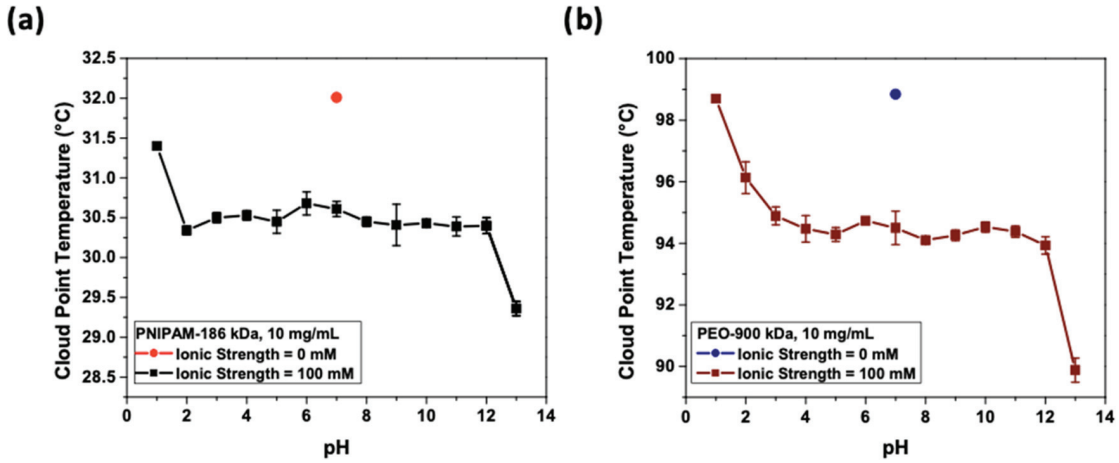

Figure 2. Cloud point of (a) 10 mg/mL PNIPAM in pure water (red data point) and 100 mM ionic strength (black data points) and (b) 10 mg/mL PEO in pure water (navy blue data point) and at 100 mM ionic strength from pH = 1.0 to 13.0 (wine red data points). The pH values listed on the *x*-axis of these graphs represent nominal values based upon adding exact concentrations of HCl or NaOH to the polymer solutions. Experimentally measured values pH are provided in Table S2.

H_3O^+ was substantially less excluded from the hydrophobic polymer interface than OH^-. Figure 1a depicts this idea schematically. The relative propensity for H_3O^+ to salt more hydrophobic thermoresponsive polymers out of solution is so modest that it should fall on the far-right side of the Hofmeister series, even beyond Ca^{2+} and Mg^{2+}. On the other hand, OH^- should be ranked between $H_2PO_4^-$ and SO_4^{2-}. Figure 1b–d depicts the chemical structures of the molecules that were studied: (1b) PNIPAM, (1c) a small molecule analogue of the PNIPAM monomer that was used in MD simulations along with a 5-mer, and (1d) PEO.

MATERIALS AND METHODS

Materials. Hydronium Chloride (HCl, ACS reagent, 37%), sodium chloride (NaCl, ≥99.5%), and sodium hydroxide (NaOH, ≥97.0%) were purchased from Sigma-Aldrich (St. Louis, MO). Poly(*N*-isopropylacrylamide) (PNIPAM; M_W = 186,800; M_w/M_n = 2.63) was purchased from Polymer Source Inc. (Quebec, Canada). Poly(ethylene oxide) (PEO-20k) (M_v ∼ 900,000) was purchased from Sigma-Aldrich (St. Louis, MO). The appropriate concentration of polymer and salt were prepared in 18.2 MΩ·cm deionized water obtained from a NANOpure Ultrapure Water System (18.2 MΩ·cm, Barnstead, Dubuque, IA). All solutions were prepared without further purification.

Cloud Point Measurements. An automated melting point apparatus (OptiMelt MPA 100, Stanford Research Systems, Sunnyvale, CA) was used to measure the turbidity in 10 mg/mL PNIPAM or PEO at the desired salt concentration. Samples were placed into capillary tubes were purchased from Kimble Chase LLC (Vineland, NJ) and had dimensions of 1.5–1.8 mm × 90 mm. The temperature of the solution was ramped at 1 °C/min from a clear solution at lower temperatures until the solution hit its cloud point temperature. An average of triplicates from three independently made solutions were used to determine the cloud point temperature of each solution.

NMR. A 500 MHz spectrometer (Bruker AVIII-HD-500) was used to take ^{1}H NMR spectra as described previously.[S1] The chemical shift of the CH_3 and CH of PNIPAM and CH_2 of PEO were monitored at 25 °C. The polymers were placed into solutions containing either pure water or a 100 mM ionic strength of HCl, NaCl, and NaOH to obtain the desired pH.

pH Measurements. The pH of experimental solutions were measured with a Thermo Orion 3 Star Benchtop pH Meter, which was calibrated by buffer solutions at pH 4, 7, and 10.

MD Simulation. Isobaric–isothermal (*NpT*) molecular dynamics (MD) simulations were performed to compute the Setschenow coefficients of HCl, NaCl, and NaOH for NIPPA (monomer) and an isotactic PNIPAM (5-mer) and the radial distribution functions of ions around interaction sites of solutes in water. A cubic simulation cell under the standard periodic boundary conditions was employed. Prior to each production MD run, isothermal-isochoric (*NVT*) and *NpT* MD simulations were performed. The time step was set to 1 fs for all simulations and the temperature and pressure were 300 K and 1 bar, respectively. Each system consists of one solute molecule, either the monomer or the 5-mer, N_w water molecules, and N_i pairs of cations and anions, where N_w = 2000 and N_i = 36 for the monomer solutions and N_w = 4000 and N_i = 72 for 5-mer solutions. For solutions with HCl, N_w was reduced by N_i because N_i water molecules and N_i protons form N_i H_3O^+ ions. The electrolyte concentration for each solution is then 1.0 mol per kg of water. We employed the TIP4P/2005 force field for water, OPLS-AA[52–54] for the NIPPA monomer and 5-mer, and the scaled-charge force field developed by Jungwirth and co-workers[55] for Na^+ and Cl^- and scaled-charge models for H_3O^+ and OH^- derived from the models developed by Netz and co-workers.[56] The choice of force field for the hydronium ions are discussed more in detail in Choice of Force Field for Acid Cation Simulations section (p.S11 in the SI).

RESULTS

Cloud Point Measurements. Figure 2a shows the cloud point temperature of 10 mg/mL PNIPAM in water as a function of pH at a constant ionic strength of 100 mM (black data points). The solutions were prepared down to pH = 1.0 by incrementally replacing NaCl by HCl. After this, the pH was raised incrementally above 7.0 by replacing NaCl with NaOH until it reached pH 13.0 at 100 mM NaOH (see

https://doi.org/10.1021/acs.jpcb.4c05748
J. Phys. Chem. B 2025, 129, 726–735

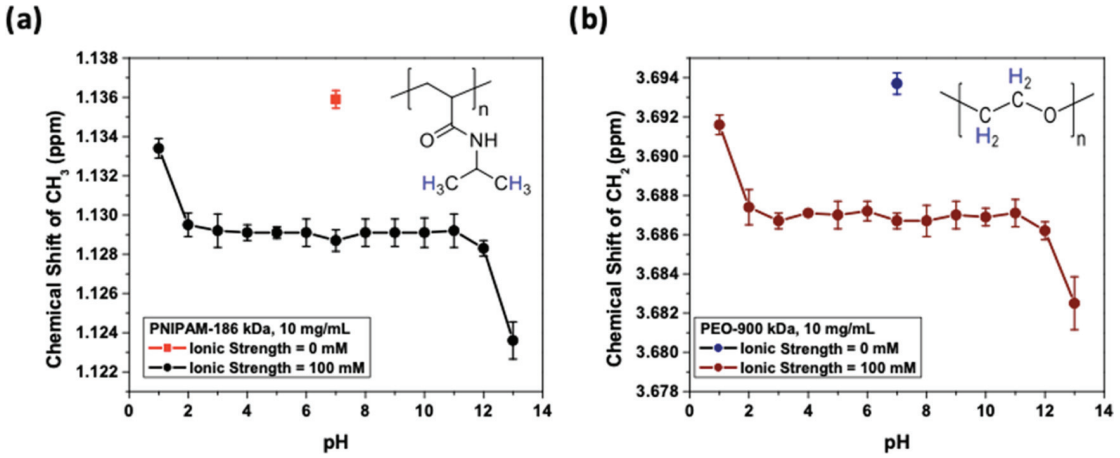

Figure 3. (a) Chemical shift of the CH_3 groups on PNIPAM in pure water (red data point) and at 100 mM strength of HCl, NaCl, and NaOH (black data points) and (b) the chemical shift of the CH_2 groups on PEO in pure water (blue data point) and at 100 mM strength with mixtures of HCl, NaCl, and NaOH (brown data points) from pH = 1 to 13.

Experimental Sample Preparation section, pS1 in the SI and Table S1 for more details on sample preparation). The red data point represents the phase transition temperature in neat water (note: the neat water solution is slightly acidic under these conditions because of dissolved CO_2, see Apparent pH vs Measured pH section, p.S2 in the SI and Table S2). As can be seen, the introduction of 100 mM NaCl lowered the cloud point by approximately 1.4 °C vs neat water (32.0 vs 30.6 °C for the black data point at a nominal pH of 7.0). Moreover, the cloud point temperatures between pH 2.0 and 12.0 remained at 30.5 ± 0.2 °C. Significantly, this value rose to 31.4 ± 0.1 °C at pH = 1.0 but fell to 29.4 ± 0.1 °C at pH = 13.0.

The 0.9 °C increase in the cloud point temperature at pH 1.0 compared to its average value between pH 2.0 to 12.0 is consistent with the notion that H_3O^+ is less depleted from the PNIPAM/water interface than Na^+. Nevertheless, HCl should be depleted from the polymer/water interface compared to the bulk solution since the cloud point was still approximately 0.6 °C lower in the former case. By contrast, the cloud point temperature at pH 13.0 was approximately 1.1 °C lower than the values between pH 2.0 and 12.0 and about 2.6 °C lower than the neat water value. As such, NaOH should be more depleted from the polymer water interface compared to either NaCl or HCl. Moreover, OH^- should be more depleted from the polymer/water interface than Cl^-.

As noted above, the pK_A of the amide oxygen is close to −0.5.[48] As such, a small fraction of the amide moieties could have possibly become protonated at pH 1.0, which would provide an alternative explanation for the increase in the cloud point temperature at pH 1.0. Therefore, an identical set of experiments was performed with PEO in place of PNIPAM under otherwise identical conditions (Figure 2b). PEO was chosen because the propensity to protonate the ether oxygen at pH 1.0 is substantially weaker than the amide oxygen.[49] In this case, the cloud point of PEO in neat water occurred near 98.8 °C (blue data point). It fell to approximately 94.5 ± 0.3 °C between pH 3.0 and 12.0 but rose to 96.1 ± 0.3 °C at pH 2.0 and to 98.7 °C ± 0.5 at pH 1.0. On the other hand, it dropped to 89.9 ± 0.3 °C at pH 13.0. These results, although shifted upward in temperature with respect to PNIPAM, are essentially analogous. As such, the PEO data are consistent with the idea that the rise in the cloud point temperature at low pH values is due to less depletion of H_3O^+ from the polymer/water interface compared to Na^+.

It should be noted that the data for PEO is more sensitive to the addition to NaCl, HCl, and NaOH compared with PNIPAM. In fact, the cloud point temperature varied by 8.9 °C between neat water and 100 mM NaOH compared to only 2.6 °C for PNIPAM. This greater sensitivity to salt may reflect the greater number of broken hydrogen bonds near the cloud point temperature of PEO compared to PNIPAM. Indeed, the PEO solutions display cloud point temperatures just a few degrees below the boiling point of water. Under these circumstances, the enrichment or depletion of the ions at the polymer/water interface became more pronounced. The fact that the cloud point temperature at pH 2.0 was clearly above the value between pH 3.0 and 12.0 should represent another manifestation of this phenomenon.

NMR Measurements. ^{1}H NMR spectroscopy was employed to follow the chemical shift of the hydrogen atoms on PNIPAM's methyl groups using the identical solution chemistries employed to measure the cloud point temperatures (Figure 3a). In this case, the measurements were made at a constant temperature of 25 °C, which was below the cloud point temperature of PNIPAM under all conditions. Analogous to the results shown in Figure 2a, the red data point just below 1.136 ppm represents the chemical shift before salt was added. As can be seen, the chemical shift moved downfield to near 1.129 between pH 2.0 and 12.0. However, it went back upfield to 1.133 ppm at pH 1.0, but further downfield to 1.124 ppm at pH 13.0. A similar set of ^{1}H NMR experiments were also performed with PEO using the hydrogen atoms on the methylene groups (Figure 3b). Again, the experiments were performed at 25 °C and the results were essentially analogous to those for PNIPAM with the ^{1}H resonance shifting downfield at pH 1.0 and upfield at pH 13.0.

The ^{1}H NMR shifts found in Figure 3 for PNIPAM and PEO resulted from changes in chain conformation rather than direct interactions between the ions and the polymer chains.[51,57,58] Indeed, even ions that interact relatively strongly with thermoresponsive polymers, like SCN^- or I^-, lead to changes in the chemical shift that are still dominated by conformational changes rather than by polymer-ion interactions. Moreover, salts that show net depletion from the polymer/water interface give rise to upfield shifts in the ^{1}H

https://doi.org/10.1021/acs.jpcb.4c05748
J. Phys. Chem. B 2025, 129, 726−735

NMR signal from CH moieties that come exclusively from conformational changes (see Polymer Conformational Changes measured by NMR section, p. S3 in the SI for details). Of course, the chemical shifts from salts that are net depleted from the polymer/water interface are still ion specific with better hydrated ions causing larger upfield shifts at a given salt concentration compared to salts that are less depleted. Indeed, NaCl, HCl, and NaOH each caused the chemical shift to move upfield compared to the neat water system. Moreover, the order of the chemical shifts, HCl < NaCl < NaOH, was consistent with the relative depletion for each salt inferred from the thermodynamic data in Figure 2. As such, the downfield shifts in Figure 3 upon substituting Na^+ with H_3O^+ were consistent with a more swollen, better hydrated chain. This occurred because Na^+ was relatively more depleted than H_3O^+. By contrast, the upfield shifts that were found upon substituting Cl^- with OH^- were consistent with a less swollen and less hydrated polymer chain, albeit one that was still well below the cloud point temperature at 25 °C for both PNIPAM and PEO. It should be noted that the net changes in the chemical shifts were quite close for the two polymers.

Next, the chemical shift for PEO remained constant from pH 11 to pH 2.0 (Figure 3b). This was different from the cloud point data in Figure 2b where the phase transition temperature already increased at pH 2. In fact, the magnitude of change in the chemical shift for PNIPAM and PEO were nearly identical in Figure 3a,b at 25 °C compared to the larger range in ΔT values seen in Figure 2b compared to Figure 2a. The differences in Figures 2b and 3b cannot arise from differences in protonation, as it is actually easier to pronate ethers at lower temperatures compared to higher temperatures.[50] As such, the more pronounced influence of pH 1.0 and 2.0 on PEO at high temperature (Figure 2b) should be the result of greater H_3O^+ accumulation around the polymer above 95 °C compared to the analogous behavior at 25 °C. Moreover, the nearly identical magnitudes of change in the chemical shift values in Figure 3a,b are remarkable given the fact that the protonation of small molecule amides occurs at a value that is three pH units higher than that of ethers.[48−50] This suggests that PNIPAM is significantly more difficult to protonate compared to small molecule amide analogues. Indeed, the polymer cannot even be protonated at pH 0, as confirmed by infrared experiments (Figure S7).

Setschenow Coefficients. Molecular dynamics (MD) simulations were performed to obtain a molecular level picture related to how NaCl, HCl, and NaOH ions influenced polymer solubility. For this purpose, both an *N*-isopropylacrylamide monomer analogue (Figure 1c) and a 5-mer of the PNIPAM chain were employed (chemical structure shown in Figure 5a, also see Simulation Detail section, p.S3 in SI for details). The ion distribution profiles with respect to PNIPAM were used to calculate Setschenow coefficient (K_s) values, which described how polymer solubility changed as the concentration of dissolved salt was increased. Experimentally, the Setschenow coefficient can be determined by using

$$\log\frac{S}{S_0} = -K_s \cdot c_s \tag{1}$$

where S is the solubility of the polymer at a given salt concentration, S_0 is its solubility in the absence of salt, and c_s is the molar concentration of salt in the bulk solution. Equivalently, K_s can be defined as the derivative of μ^*, the solvation free energy of the polymer in an electrolyte solution with respect to c_s, at constant temperature and pressure

$$K_S = \left(\frac{\partial \mu^*/RT}{\partial c_s}\right)_{T,p} \tag{2}$$

where R is the gas constant and T is the absolute temperature. The change in μ^* with salt concentration at low salt concentrations is related to the difference in the Kirkwood−Buff integrals for the ion-polymer and water−polymer pair correlation functions (see Kirkwood−Buff (KB) Integral, Figure S2 in SI for details).[59] The corresponding values are readily obtained from MD simulations (see Setschenow coefficient K_s, Figure S3). A positive K_s value indicates that the polymer chain is made less soluble as c_s is increased, while a negative value corresponds to increased solubility.

K_s values for both the *N*-isopropylacrylamide monomer (purple) and PNIPAM 5-mer (green) are provided in Figure 4.

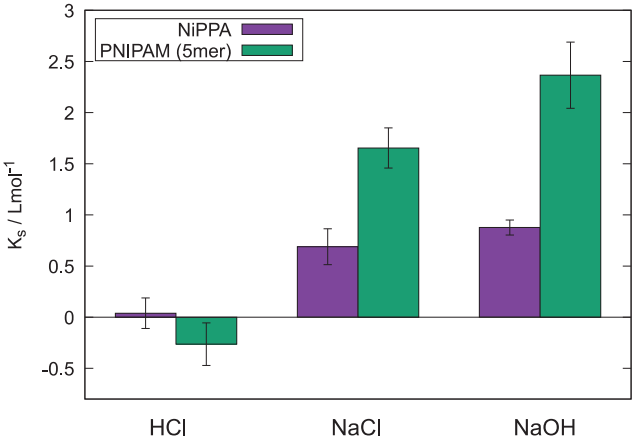

Figure 4. Setschenow coefficients K_s of three electrolytes, HCl, NaCl, and NaOH, for NIPPA (monomer) and PNIPAM (5-mer).

It should be noted that the values were derived from MD simulations of aqueous solutions of 1 M HCl, 1 M NaCl, and 1 M NaOH, which corresponds to pH = 0, 7.0, and 14, respectively. The acid and base concentrations were an order of magnitude larger than those used in the experiments but were used because they provided better statistics for the correlation functions. As shown in the bar graphs in Figure 4, the K_s values for HCl were very close to zero, which indicated that the simulations predicted neither depletion nor enrichment at the monomer or 5-mer/water interface. The salting out behavior, however, was clearly pronounced for NaCl, and this behavior was even stronger with NaOH. Moreover, the fact that the 5-mer was more strongly salted out by both NaCl and NaOH is in line with the general trend that larger solutes tend to yield more positive K_s values in a homologous series of solutes with a given salt.[60] The results in Figure 4 were also in good agreement with the cloud point data and ^{1}H NMR measurements shown above, although the experiments indicated a very small salting out effect for HCl, rather than a neutral or very small salting in effect. This difference may be due to the higher HCl concentration utilized in MD simulations or due to the combination of the force fields for water, ions, and PNIPAM 5-mer.

Radial Distribution Functions (RDFs). Next, we examined the RDFs, $g(r)$, for the PNIPAM 5-mer (Figure

https://doi.org/10.1021/acs.jpcb.4c05748
J. Phys. Chem. B 2025, 129, 726−735

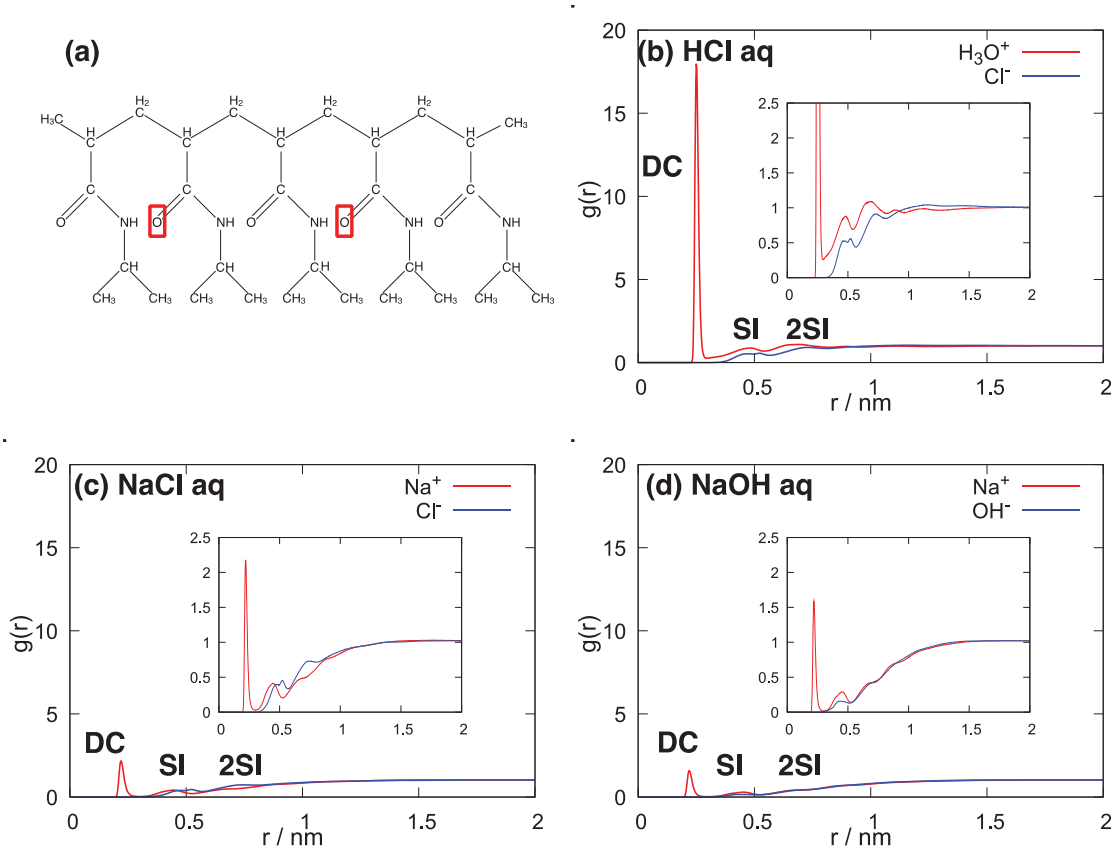

Figure 5. RDF of the cation (red) and anion (blue) from the penultimate amide oxygen (a) in solutions of (b) 1 M HCl, (c) 1 M NaCl, and (d) 1 M NaOH. The locations on the graph are labeled as follows: an ion direct contact with the amide oxygen (DC) on the PNIPAM-5mer, a solvent-shared ion (SI) interaction, and a solvent-separated ion (2SI) interaction.

5a). Figure 5b–d shows results for the distribution functions of both cations and anions with respect to the penultimate carbonyl oxygens, highlighted by the red boxes in Figure 5a. Specifically, Figure 5b shows the curves for H_3O^+ (red curve) and Cl^- (blue curve). For H_3O^+, *r* indicates the O–O distance. These particular atomic positions were selected because they were associated with the strongest ion-oligomer interactions. RDFs for other positions along the 5-mer are provided in the Supporting Information (see Radial Distribution Functions (RDF) section, Figures S4–S6). As can be seen, H_3O^+ was strongly enriched near 0.25 nm, which represents nearest neighbor contact of H_3O^+ with the carbonyl oxygen. The much smaller peaks near 0.5 and 0.7 nm, corresponding to solvent-shared (SI) and a solvent-separated (2SI) interactions, are highlighted on an enlarged scale in the inset. In contrast with H_3O^+, the Cl^- counterion was excluded from the carbonyl oxygens. Next, the RDFs with 1 M NaCl showed less pronounced cation interactions (Figure 5c). In this case, Na^+ (red curve) was modestly enriched at the penultimate carbonyl oxygens, while Cl^- (blue curve) was excluded from this position and hardly differed from the Cl^- data when H_3O^+ was the counterion. Finally, the OH^- anion was more strongly depleted from the solute (Figure 5d, blue curve) in 1 M NaOH than Cl^- was at this same carbonyl oxygen position. Moreover, the modest peak for Na^+ at 0.25 nm (red curve) was substantially smaller than it was in Figure 5b with Cl^- as the counterion.

DISCUSSION

The central question to address here is the placement of H_3O^+ and OH^- in the cationic and anionic Hofmeister series, respectively. Previous literature has shown that both monovalent and divalent metal cations are depleted from the PNIPAM/water interface when the counteranion is chloride.[61] Locally, however, Mg^{2+} can partition together with Cl^- to the amide oxygen to form a solvent-shared configuration. Ca^{2+} and Li^+ can do this as well, but to a lesser extent. On the other hand, more weakly hydrated monovalent cations, including Na^+, K^+, Rb^+, and Cs^+, are even more strongly depleted from the amide oxygen.

The data in Figure 2a demonstrate that 100 mM HCl causes the cloud point temperature of PNIPAM to decrease by 0.6 °C compared to pure water. By comparison, 100 mM $MgCl_2$ decreases the cloud point by a little more than 1.2 °C, while 100 mM $CaCl_2$ decreases it by 1.5 °C.[61] Of course, both Ca^{2+} and Mg^{2+} are divalent metal cations and are present in solution together with 200 mM Cl^-. Since the temperature drop with $CaCl_2$ is more than twice as large, H_3O^+ can be unambiguously placed to the right of Ca^{2+} in the Hofmeister series. The comparison between H_3O^+ and Mg^{2+} is slightly more complicated. However, unless one were to assign 100% of the decrease to Cl^-, H_3O^+ should be to the right of Mg^{2+} too. Indeed, according to simulations, Mg^{2+} is strongly excluded from the PNIPAM/water interface until it forms an ion pair with Cl^-.[61] As such, unpaired Mg^{2+} should help salt the polymer out. Interestingly, there is no evidence that H_3O^+ and Cl^- form an ion pair, as the former approaches the polymer. As

https://doi.org/10.1021/acs.jpcb.4c05748
J. Phys. Chem. B 2025, 129, 726–735

such, H_3O^+ should almost certainly be placed to the right of Mg^{2+} (Figure 1a).

Next, the data shown above makes it clear that OH^- is more excluded than Cl^- from the polymer/water interface. Specifically, 100 mM NaOH lowers the cloud point of PNIPAM by 2.6 °C (Figure 2a). By comparison, the values for NaF and NaH_2PO_4 are both less than 2 °C.[61,62] As such, OH^- should be more strongly excluded from the PNIPAM/water interface than any other standard monovalent Hofmeister anion. By contrast, 100 mM Na_2SO_4 depresses the PNIPAM cloud point by more than 3 °C. One certainly should be concerned with the fact that there are 200 mM Na^+ cations when SO_4^{2-} is the counterion. However, cation identity generally has a far less pronounced influence on the cloud point of PNIPAM than anion identity. This suggests that OH^- is not quite as well excluded as SO_4^{2-}. As such, it is appropriate to place it between $H_2PO_4^-$ and SO_4^{2-} in the anionic Hofmeister series (Figure 1a). It should be noted that OH^- is located at the same position in the anionic Hofmeister series for PNIPAM as it is for the air/water interface.[10] By contrast, H_3O^+ is different because the cationic Hofmeister series at the air/water interface is largely reversed from the series for thermoresponsive polymers.[10,31,61,63] Remarkably, H_3O^+ falls all the way to right in both series, as it is the least excluded cation in both cases.

The placement of H_3O^+ and OH^- at the extreme ends of at least their respective monovalent Hofmeister ion series is curious. This ordering raises questions as to why the behavior of uncharged thermoresponsive polymers can be more influenced by these two ions compared to others. One difference should involve the way H_3O^+ and OH^- are solvated. Specifically, other cations and anions (e.g., Mg^{2+} and Ca^{2+} or $H_2PO_4^-$ and SO_4^{2-}) disrupt the hydrogen bonding network to a greater extent than H_3O^+ and OH^-. By contrast, H_3O^+ and OH^-, are directly integrated into the hydrogen bonding network and diffuse through water via the Grotthuss mechanism.[64] Other ions can only diffuse through water by vehicular diffusion.

Despite their seeming similarities, there are significant differences between hydronium and hydroxide ions that need to be considered. Recent studies suggest that the Eigen form of the hydronium ion, which consists of H_3O^+ hydrogen bond to three waters to form $H_9O_4^+$, is not particularly stable in aqueous solutions.[65] Also, the Zundel cation, which equally shares the proton between two adjacent water molecules ($H_5O_2^+$), is not a stable configuration either.[66−68] Instead, the proton appears to exist in a near continuum of configurations between the Eigen and Zundel extremes, which are neither completely covalently bound to a single water molecule, nor equally shared between two adjacent water molecules. By contrast, OH^- is a relatively stable species in aqueous solutions. Calculations suggest that hydroxide's OH bond is a poor hydrogen bond donor, but that its oxygen atom is hyper coordinated to four or more adjacent water molecules, rather than just three.[64] A second key difference between H_3O^+ and OH^- concerns the nature of the counterions. At concentrations of 100 mM and above, H_3O^+ is never more than a few nanometers from a counter Cl^- anion, while OH^- is never more than a few nanometers from a Na^+ countercation. As such, ion pairing needs to be considered. Indeed, the interactions between H_3O^+ and Cl^- are weaker than those between Na^+ and OH^-.[69] It should be a combination of the differences in the physical properties between H_3O^+ and OH^- that ultimately leads to their opposite behaviors at hydrophobic interfaces.

As noted above, unlike Mg^{2+} and Ca^{2+}, which have been shown to drag their counterions to the polymer interface,[61] H_3O^+ was not found to drag its counterion to the polymer interface (Figure 5). H_3O^+ is unique among cations as it has the capability to diffuse very rapidly through solution via the Grotthuss mechanism. Indeed, the identity of the H_3O^+ molecule can be changed by the making and breaking of hydrogen bonds. By contrast, the other cations move through solution by the slower vehicular diffusion mechanism. As such, the enhanced diffusion of hydronium may not allow the counteranion to follow it as closely as would be the case for a metal cation, which may be part of the unique behavior for hydronium ions at hydrophobic interfaces.

Finally, it should be noted that changes in the phase transition temperature of thermoresponsive polymers can be quite sensitive to specific polymer properties such as the degree of polymerization of the polymer, tacticity, end group chemistry, polydispersity, and polymer concentration. In this work, it was found that the cloud point decreased by −0.6 °C upon the addition of 100 mM HCl compared to conditions where no salt was added (Figure 2a). Curiously, Dong and coworkers recently found a much larger decrease in the phase transition temperature upon the addition of HCl under similar conditions.[70] Such a result may indicate that cloud point temperature changes upon addition of H_3O^+ are particularly sensitive to the exact polymer structure or related variables.

CONCLUSIONS

In this manuscript, H_3O^+ and OH^- ions were placed into the Hofmeister Series based on their propensities to salt hydrophobic polymers out of solution. H_3O^+ was located on the far-right side of the cation series, beyond Ca^{2+} and Mg^{2+}, while OH^- fell in between $H_2PO_4^-$ and SO_4^{2-}. A combination of thermodynamic and spectroscopic measurements as well as all-atom MD simulations were consistent with the idea that H_3O^+ was only very weakly depleted from the polymer/water interface and interacted most favorably with the amide oxygen on PNIPAM. By contrast, OH^- was strongly partitioned away from the PNIPAM polymer. These finds are mostly similar to the partitioning of the same ions at the air/water interface, where H_3O^+ is slightly enriched and OH^- is strongly excluded. In the future, it would be of interest to explore how H_3O^+ and OH^- partition at hydrophilic polymers/water interfaces, although such studies will be more challenging as polymers that display an upper critical solution temperature often have more functional groups. Also, it would be interesting to understand if there is any relationship between the strong partitioning behavior of H_3O^+/OH^- and the Grotthuss mechanism.

ASSOCIATED CONTENT

Supporting Information

The Supporting Information is available free of charge at https://pubs.acs.org/doi/10.1021/acs.jpcb.4c05748.

Experimental sample preparation; apparent pH vs measured pH; polymer conformational changes measured by NMR; simulation details; Kirkwood−Buff (KB) integral, Setschenow coefficient K_s; radial distribution functions (RDFs); and infrared data (PDF)

https://doi.org/10.1021/acs.jpcb.4c05748
J. Phys. Chem. B 2025, 129, 726−735

AUTHOR INFORMATION

Corresponding Authors

Kenichiro Koga − *Department of Chemistry, Okayama University, Okayama 700-8530, Japan; Research Institute for Interdisciplinary Science, Okayama University, Okayama 700-8530, Japan;* orcid.org/0000-0002-1153-5831; Email: koga@okayama-u.ac.jp

Paul S. Cremer − *Department of Chemistry, The Pennsylvania State University, University Park, Pennsylvania 16802, United States; Department of Biochemistry and Molecular Biology, The Pennsylvania State University, University Park, Pennsylvania 16802, United States;* orcid.org/0000-0002-8524-0438; Email: psc11@psu.edu

Authors

Ryan L. Myers − *Department of Chemistry, The Pennsylvania State University, University Park, Pennsylvania 16802, United States; Department of Chemistry, University of Pittsburgh at Bradford, Bradford, Pennsylvania 16701, United States;* orcid.org/0009-0003-1216-5486

Aoi Taira − *Department of Chemistry, Okayama University, Okayama 700-8530, Japan*

Chuanyu Yan − *Department of Chemistry, The Pennsylvania State University, University Park, Pennsylvania 16802, United States*

Seung-Yi Lee − *Department of Chemistry, The Pennsylvania State University, University Park, Pennsylvania 16802, United States*

Lauren K. Welsh − *Department of Chemistry, The Pennsylvania State University, University Park, Pennsylvania 16802, United States*

Patrick R. Ianiro − *Department of Chemistry, University of Pittsburgh at Bradford, Bradford, Pennsylvania 16701, United States*

Tinglu Yang − *Department of Chemistry, The Pennsylvania State University, University Park, Pennsylvania 16802, United States;* orcid.org/0000-0003-0872-8218

Complete contact information is available at: https://pubs.acs.org/10.1021/acs.jpcb.4c05748

Author Contributions

#R.L.M. and A.T. contributed equally to this work.

Notes

The authors declare no competing financial interest.

ACKNOWLEDGMENTS

P.S.C. thanks the National Science Foundation for funding, NSF CHE-2305129. K.K. thanks KAKENHI (Grant Numbers 18KK0151 and 20H02696). Part of the computation was performed using Research Center for Computational Science, Okazaki, Japan (Project: 22-IMS-C124, 23-IMS-C112). AT thanks JST, the establishment of university fellowships towards the creation of science technology innovation, Grant Number JPMJFS2128.

REFERENCES

(1) Hofmeister, F. On the understanding of the effects of salts. *Naunyn-Schmiedeberg's Arch. Pharmacol.* **1888**, *24*, 247−260.

(2) Pinna, M. C.; Bauduin, P.; Touraud, D.; Monduzzi, M.; Ninham, B. W.; Kunz, W. Hofmeister effects in biology: effect of choline addition on the salt-induced super activity of horseradish peroxidase and its implication for salt resistance of plants. *J. Phys. Chem. B* **2005**, *109*, 16511−16514.

(3) Pinna, M. C.; Salis, A.; Monduzzi, M.; Ninham, B. W. Hofmeister series: the hydrolytic activity of Aspergillus niger lipase depends on specific anion effects. *J. Phys. Chem. B* **2005**, *109*, 5406−5408.

(4) Bauduin, P.; Nohmie, F.; Touraud, D.; Neueder, R.; Kunz, W.; Ninham, B. W. Hofmeister specific-ion effects on enzyme activity and buffer pH: Horseradish peroxidase in citrate buffer. *J. Mol. Liq.* **2006**, *123*, 14−19.

(5) Vrbka, L.; Jungwirth, P.; Bauduin, P.; Touraud, D.; Kunz, W. Specific ion effects at protein surfaces: a molecular dynamics study of bovine pancreatic trypsin inhibitor and horseradish peroxidase in selected salt solutions. *J. Phys. Chem. B* **2006**, *110*, 7036−7043.

(6) Baldwin, R. L. How Hofmeister Ion Interactions Affect Protein Stability. *Biophys. J.* **1996**, *71* (4), 2056−2063.

(7) Zhang, Y.; Furyk, S.; Bergbreiter, D. E.; Cremer, P. S. Specific Ion Effects on the Water Solubility of Macromolecules: PNIPAM and the Hofmeister Series. *J. Am. Chem. Soc.* **2005**, *127* (41), 14505−14510.

(8) Zhang, Y.; Cremer, P. S. Interactions between macromolecules and ions: the Hofmeister series. *Curr. Opin. Chem. Biol.* **2006**, *10*, 658−663.

(9) Flores, S. C.; Kherb, J.; Konelick, N.; Chen, X.; Cremer, P. S. The Effects of Hofmeister Cations at Negatively Charged Hydrophilic Surfaces. *J. Phys. Chem. C* **2012**, *116*, 5730−5734.

(10) Pegram, L. M.; Record, M. T. Hofmeister salt effects on surface tension arise from partitioning of anions and cations between bulk water and the air−water interface. *J. Phys. Chem. B* **2007**, *111*, 5411−5417.

(11) Sthoer, A.; Tyrode, E. Interactions of Na^+ Cations with a Highly Charged Fatty Acid Langmuir Monolayer: Molecular Description of the Phase Transition. *J. Phys. Chem. C* **2019**, *123*, 23037−23048.

(12) Healy, T. W.; White, L. R. Ionizable surface group models of aqueous interfaces. *Adv. Colloid Interface Sci.* **1978**, *9* (4), 303−345.

(13) Dynarowicz-Latka, P.; Cavalli, A.; Oliveira, O. N., Jr Dissociation constants of aromatic carboxylic acids spread at the air/water interface. *Thin Solid Films* **2000**, *360* (1−2), 261−267.

(14) González-Jiménez, M.; Liao, Z.; Williams, E. L.; Wynne, K. Lifting Hofmeister's Curse: Impact of Cations on Diffusion, Hydrogen Bonding, and Clustering of Water. *J. Am. Chem. Soc.* **2024**, *146*, 368−376.

(15) Jenkins, H. D. B.; Marcus, Y. Viscosity B-Coefficients of Ions in Solution. *Chem. Rev.* **1995**, *95* (8), 2695−2724.

(16) Vácha, R.; Zangi, R.; Engberts, J. B. F. N.; Jungwirth, P. Water Structuring and Hydroxide Ion Binding at the Interface between Water and Hydrophobic Walls of Varying Rigidity and van der Waals Interactions. *J. Phys. Chem. C* **2008**, *112* (20), 7689−7692.

(17) Gopalakrishnan, S.; Liu, D. F.; Allen, H. C.; Kuo, M.; Shultz, M. J. Vibrational spectroscopic studies of aqueous interfaces: salts, acids, bases, and nanodrops. *Chem. Rev.* **2006**, *106*, 1155−1175.

(18) Mucha, M.; Frigato, T.; Levering, L. M.; Allen, H. C.; Tobias, D. J.; Dang, L. X.; Jungwirth, P. Unified molecular picture of the surfaces of aqueous acid, base, and salt solutions. *J. Phys. Chem. B* **2005**, *109*, 7613−7623.

(19) Tarbuck, T. L.; Ota, S. T.; Richmond, G. L. Spectroscopic Studies of Solvated Hydrogen and Hydroxide Ions at Aqueous Surfaces. *J. Am. Chem. Soc.* **2006**, *128*, 14519−14527.

(20) Gilbert, H. W.; Shaw, P. E. Electrical charges arising at a liquid-gas interface. *Proc. Phys. Soc. London* **1924**, *37*, No. 195.

(21) Graciaa, A.; Morel, G.; Saulner, P.; Lachaise, J.; Schechter, R. S. The ζ-Potential of Gas Bubbles. *J. Colloid Interface Sci.* **1995**, *172*, 131−136.

(22) Takahashi, M. ζ Potential of Microbubbles in Aqueous Solutions: Electrical Properties of the Gas−Water Interface. *J. Phys. Chem. B* **2005**, *109*, 21858−21864.

(23) Beattie, J. K.; Djerdjev, A. M. The pristine oil/water interface: surfactant-free hydroxide-charged emulsions. *Angew. Chem., Int. Ed.* **2004**, *43*, 3568−3571.

(24) Beattie, J. K. The intrinsic charge on hydrophobic microfluidic substrates. *Lab Chip* **2006**, *6*, 1409−1411.
(25) Beattie, J. K. *Colloid Stability: The Role of Surface Forces, Part II*; Tadros, T. F., Ed.; Wiley: Weinheim, 2006; p 153.
(26) Creux, P.; Lachaise, J.; Graciaa, A.; Beattie, J. K.; Djerdjev, A. M. Strong specific hydroxide ion binding at the pristine oil/water and air/water interfaces. *J. Phys. Chem. B* **2009**, *113*, 14146−14150.
(27) dos Santos, A. P.; Levin, Y. Surface Tensions and Surface Potentials of Acid Solutions. *J. Chem. Phys.* **2010**, *133* (15), No. 154107.
(28) Das, S.; Bonn, M.; Backus, E. H. G. The Surface Activity of the Hydrated Proton is Substantially Higher than That of the Hydroxide Ion. *Angew. Chem., Int. Ed.* **2019**, *58* (44), 15636−15639.
(29) Chiang, K.-Y.; Dalstein, L.; Wen, Y. Affinity of Hydrated Protons at Intrinsic Water/Vapor Interface Revealed by Ion-Induced Water Alignment. *J. Phys. Chem. Lett.* **2020**, *11* (3), 696−701.
(30) Weissenborn, P. K.; Pugh, R. J. J. Surface Tension of the Aqueous Solutions of Electrolytes. *J. Colloid Interface Sci.* **1996**, *184*, 550−563.
(31) Jarvis, N. L.; Scheiman, M. A. Surface Potentials of Aqueous Electrolyte Solutions. *J. Phys. Chem. A* **1968**, *72* (1), 74−78.
(32) Bredt, A. J.; Kim, Y.; Mendes de Oliveira, D.; Urbina, A. S.; Slipchenko, L. V.; Ben-Amotz, D. Ion Correlations Explain Solute-Dependent Changes in Water Structure. *J. Phys. Chem. B* **2022**, *126* (4), 869−877.
(33) Winter, B.; Faubel, M. Photoemission from Liquid Aqueous solution. *Chem. Rev.* **2006**, *106*, 1176−1211.
(34) Petersen, P. B.; Saykally, R. J. Adsorption of Ions to the Surface of Dilute Electrolyte Solutions: The Jones−Ray Effect Revisited. *J. Phys. Chem. B* **2005**, *109*, 7976−7980.
(35) Petersen, P. B.; Saykally, R. J. On the nature of ions at the liquid water surface. *Annu. Rev. Phys. Chem.* **2006**, *57*, 333−364.
(36) Petersen, P. B.; Saykally, R. J. Is the liquid water surface basic or acidic? Macroscopic vs. molecular-scale investigations. *Chem. Phys. Lett.* **2008**, *458*, 255−261.
(37) Buch, V.; Milet, A.; Vacha, R.; Jungwirth, P.; Devlin, J. P. Water surface is acidic. *Proc. Natl. Acad. Sci. U.S.A.* **2007**, *104*, 7342−7347.
(38) Bergeron, V.; Waltermo, A.; Claesson, P. M. Disjoining Pressure Measurements for Foam Films Stabilized by a Nonionic Sugar-Based Surfactant. *Langmuir* **1996**, *12*, 1336−1342.
(39) Karraker, K. A.; Radke, C. J. Disjoining pressures, zeta potentials and surface tensions of aqueous non-ionic surfactant/electrolyte solutions: theory and comparison to experiment. *Adv. Colloid Interface Sci.* **2002**, *96*, 231−264.
(40) Stubenrauch, C.; von Klitzing, R. Disjoining pressure in thin liquid foam and emulsion films—new concepts and perspectives. *J. Phys.: Condens. Matter* **2003**, *15*, No. R1197.
(41) Petersen, M. K.; Iyengar, S. S.; Day, T. J. F.; Voth, G. A. The Hydrated Proton at the Water/Liquid Vapor Interface. *J. Phys. Chem. B* **2004**, *108*, 14804−14806.
(42) Swanson, J. M. J.; Mauphin, C. M.; Chen, H.; Petersen, M. K.; Xu, J.; Wu, Y.; Voth, G. A. Proton solvation and transport in aqueous and biomolecular systems: insights from computer simulations. *J. Phys. Chem. B* **2007**, *111*, 4300−4314.
(43) Tse, Y.-L. S.; Chen, C.; Lindberg, G. E.; Kumar, R.; Voth, G. A. Propensity of Hydrated Excess Protons and Hydroxide Anions for the Air−Water Interface. *J. Am. Chem. Soc.* **2015**, *137* (39), 12610−12616.
(44) Baer, M. D.; Kuo, I-F. W.; Tobias, D. J.; Mundy, C. J. Toward a unified picture of the water self-ions at the air-water interface: a density functional theory perspective. *J. Phys. Chem. B* **2014**, *118* (28), 8364−8372.
(45) Mondal, J. A.; Namboodiri, V.; Mathi, P.; Singh, A. K. Alkyl Chain Length Dependent Structural and orientational transformations of water at alcohol-water interfaces and its relevance to atmospheric aerosols. *J. Phys. Chem. Lett.* **2017**, *8* (7), 1637−1644.
(46) Wen, Y.; Zha, S.; Tian, C.; Shen, Y. R. Surface pH and Ion Affinity of the Alcohol-Monolayer/Water Interface Studied by Sum-Frequency Spectroscopy. *J. Phys. Chem. C* **2016**, *120* (28), 15224−15229.
(47) Fang, H.; Wu, W.; Sang, Y.; Chen, S.; Zhu, X.; Zhang, L.; Niu, Y.; Gan, W. The behavior of hydroxide and hydronium ions at the hexadecane-water interface studied with second harmonic generation and zeta potential measurements. *RSC Adv.* **2015**, *5*, 23578−23585.
(48) Grant, H. M.; Mctigue, P.; Ward, D. G. The basicities of aliphatic amides. *Aust. J. Chem.* **1983**, *36* (11), 2211−2218.
(49) Deno, N. C.; Turner, J. O. The basicity of Alcohols and Ethers. *J. Org. Chem.* **1966**, *31* (6), 1969−1970.
(50) Perdoncin, G.; Scorrano, G. Protonation Equilibria in Water at Several Temperatures of Alcohols, Ethers, Acetone, Dimethyl Sulfide, and Dimethyl Sulfoxide. *J. Am. Chem. Soc.* **1977**, *99* (21), 6983−6986.
(51) Rogers, B. A.; Okur, H. I.; Yan, C.; Yang, T.; Heyda, J.; Cremer, P. S. Weakly hydrated anions bind to polymers but not monomers in aqueous solution. *Nat. Chem.* **2022**, *14*, 40−45.
(52) Jorgensen, W. L.; Tirado-Rives, J. Potential energy functions for atomic-level simulations of water and organic and biomolecular systems. *Proc. Natl. Acad. Sci. U.S.A.* **2005**, *102*, 6665−6670.
(53) Dodda, L. S.; Vilseck, J. Z.; Tirado-Rives, J.; Jorgensen, W. L. 1.14*CM1A-LBCC: Localized Bond-Charge Corrected CM1A Charges for Condensed-Phase Simulations. *J. Phys. Chem. B* **2017**, *121* (15), 3864−3870.
(54) Dodda, L. S.; de Vaca, I. C.; Tirado-Rives, J.; Jorgensen, W. L. LigParGen web server: an automatic OPLS-AA parameter generator for organic ligands. *Nucleic Acids Res.* **2017**, *45*, W331−W336.
(55) Kohagen, M.; Mason, P. E.; Jungwirth, P. Accounting for electronic polarization effects in aqueous sodium chloride via molecular dynamics aided by neutron scattering. *J. Phys. Chem. B* **2016**, *120* (8), 1454−1460.
(56) Bonthuis, D. J.; Mamatkulov, S. I.; Netz, R. R. Optimization of classical nonpolarizable force fields for OH^- and H_3O^+. *J. Chem. Phys.* **2016**, *144* (10), No. 104503.
(57) Rembert, K. B.; Paterová, J.; Heyda, J.; Hilty, C.; Jungwirth, P.; Cremer, P. S. Molecular Mechanisms of Ion-Specific Effects on Proteins. *J. Am. Chem. Soc.* **2012**, *134*, 10039−10046.
(58) Rembert, K. B.; Okur, H.; Hilty, C.; Cremer, P. S. An NH Moiety is not Required for Anion Binding to Amides in Aqueous Solution. *Langmuir* **2015**, *31*, 3459−3464.
(59) Lee, L. L. A molecular theory of Setchenov's salting-out principle and applications in mixed-solvent electrolyte solutions. *Fluid Phase Equilib.* **1997**, *131*, 67−82.
(60) Katsuto, H.; Okamoto, R.; Sumi, T.; Koga, K. Ion Size Dependences of the Salting-out Effect: Reversed Order of Sodium and Lithium Ions. *J. Phys. Chem. B* **2021**, *125* (23), 6296−6305.
(61) Bruce, E. E.; Okur, H. I.; Stegmaier, S.; Drexler, C. I.; Rogers, B. A.; van der Vegt, N. F. A.; Roke, S.; Cremer, P. S. Molecular mechanism for the interactions of Hofmeister cations with macromolecules in aqueous solution. *J. Am. Chem. Soc.* **2020**, *142*, 19094−19100.
(62) Zhang, Y.; Cremer, P. S. Chemistry of Hofmeister Anions and Osmolytes. *Annu. Rev. Phys. Chem.* **2010**, *61*, 16447−16454.
(63) Sthoer, A.; Hladilkova, J.; Lund, M.; Tyrode, E. Molecular insight into carboxylic acid-alkali metal cations interactions: reversed affinities and ion-pair formation revealed by non-linear optics and simulations. *Phys. Chem. Chem. Phys.* **2019**, *21*, 11329−11344.
(64) Marx, D.; Chandra, A.; Tuckerman, M. E. Aqueous Basic Solutions: Hydroxide Solvation, Structural Diffusion, and Comparison to the Hydrated Proton. *Chem. Rev.* **2010**, *110* (4), 2174−2216.
(65) Di Pino, S.; Donkor, E. D.; Sánchez, V. M.; Rodriguez, A.; Cassone, G.; Scherlis, D.; Hassanali, A. ZundEig: The Structure of the Proton in Liquid Water from Unsupervised Learning. *J. Phys. Chem. B* **2023**, *127* (45), 9822−9832.
(66) Eigen, M.; DeMaeyer, L. Self-dissociation and protonic charge transport in water and ice. *Proc. R. Soc. London, Ser. A* **1958**, *247*, 505−533.
(67) Zundel, G. Hydration structure and intermolecular interaction in polyelectrolytes. *Angew. Chem., Int. Ed.* **1969**, *8*, 499−509.

https://doi.org/10.1021/acs.jpcb.4c05748
J. Phys. Chem. B 2025, 129, 726−735

(68) Gomez, A.; Thompson, W. H.; Laage, D. Proton Transport is doubly gated by sequential hydrogen-bond exchanges *ChemRxiv* 2024.
(69) Drexler, C. I.; Miller, T. C.; Rogers, B. A.; Li, Y. C.; Daly, C. A., Jr.; Yang, T.; Corcelli, S. A.; Cremer, P. S. Counter cations affect transport in aqueous hydroxide solutions with ion specificity. *J. Am. Chem. Soc.* **2019**, *141* (17), 6930−6936.
(70) Dong, Z.; Qu, Y.; Jiao, Y.; Xue, K.; Zhu, W.; Liu, H.; Qi, J.; Wang, Y. Temperature response behavior of poly(1-vinyl-3-methylimidazole dimethyl phosphate-co-N-isopropylacrylamide) in aqueous and ester solutions driven by hydrogen bonding. *J. Mol. Liq.* **2024**, *395*, No. 123848.

https://doi.org/10.1021/acs.jpcb.4c05748
J. Phys. Chem. B 2025, 129, 726−735